Computational Materials Science 50 (2011) 3063–3066

Contents lists available at ScienceDirect

Computational Materials Science

journal homepage: www.elsevier.com/locate/commatsci

Atomistic simulations on the mechanical properties of a silicon nanofilm covered with graphene

Yuhang Jing [a,b], N.R. Aluru [b,*]

[a] Department of Astronautical Science and Mechanics, Harbin Institute of Technology, Harbin 150001, People's Republic of China
[b] Department of Mechanical Science and Engineering, Beckman Institute for Advanced Science and Technology, University of Illinois at Urbana-Champaign, Urbana, IL 61801, USA

ARTICLE INFO

Article history:
Received 30 March 2011
Received in revised form 16 May 2011
Accepted 17 May 2011

Keywords:
Si nanofilm
Graphene
Mechanical properties
Molecular dynamics

ABSTRACT

Molecular dynamics simulations are used to investigate the mechanical properties of a silicon nanofilm covered with graphene. Our results show that graphene can enhance the mechanical properties of a silicon nanofilm. The Young's modulus of the silicon structure covered with graphene decreases as the thickness of the silicon nanofilm increases. We also investigate the fracture process of the silicon structure covered with graphene. The results in this paper suggest that silicon structures covered with graphene open up opportunities for design of micro and nanoelectromechanical systems.

1. Introduction

Mechanical properties of nanoscale structures need to be understood in detail to enable design of high-performance and reliable micro/nanoelectromechanical systems (MEMS/NEMS) [1]. Single-crystal silicon and silicon-based materials (e.g., silicon dioxide and polycrystalline silicon films) are some of the most commonly used materials in MEMS/NEMS. However, single-crystal silicon and silicon-based materials are brittle and have poor surface mechanical properties (e.g., scratch/wear tests) compared to SiC film [2]. Materials with different mechanical, thermal, and electrical properties are needed to design smart and functional MEMS/NEMS devices. Graphene, which is a two-dimensional (2D) atomic layer of graphite, forms the basis of both 3D graphite and 1D carbon nanotubes. Its intrinsic strength has been shown (from both experiments and simulations) to exceed that of other materials, thus, establishing graphene as a potential reinforcement material for next generation composite materials [3]. Huang and coworkers [4] showed that a graphene/poly(vinyl alcohol) nanocomposite leads to a 76% increase in tensile strength and a 62% improvement of Young's modulus with only 0.7 wt.% graphene oxide. Cheng and coworkers [5] reported that a freestanding and flexible graphene/polyaniline composite sheet has a tensile strength of 12.6 MPa. Zhang and coworkers [6] obtained a 150% improvement in tensile strength and a nearly 10-fold increase of Young's modulus for the graphene/poly(vinyl alcohol) composite with 1.8 vol.% graphene. Considering the above results, integration of graphene with silicon and silicon-based materials can open up opportunities for MEMS/NEMS devices. The mechanical properties of silicon nanofilms have been investigated extensively because of their applications in flexible electronics and MEMS [7–10]. Fujii and Akiniwa [11] investigated the effects of notch depth and crystal orientation on the deformation and fracture behaviour of single crystal silicon thin films. Fedorchenko et al. [12] reported that the elastic modulus of a Si nanofilm varied with film thickness based on theoretical analysis. However, the mechanical properties of silicon covered with a graphene film have not been investigated before.

2. Simulation details

In this paper, we perform a series of molecular dynamics (MD) simulations to investigate the mechanical properties of a silicon nanofilm covered with graphene. We investigate how the mechanical properties of a silicon nanofilm covered with graphene depend on the thickness of the silicon nanofilm. The thickness of the silicon nanofilm is varied from 1 to 9 nm. Molecular dynamics simulations are performed using LAMMPS [13]. We investigate several interatomic potentials in the MD simulations, including Tersoff [14], Erhart–Albe [15], AIREBO [16], and MEAM [17,18]. To study the mechanical properties of silicon nanofilms covered with graphene, we perform uniaxial tensile tests under deformation-control method by applying the strain rate in the uniaxial direction. In the deformation-control method, the applied strain rate is 0.001 ps^{-1}. The strain increment is applied to the structure after every 10,000 time steps. All the MD simulations are carried out at

* Corresponding author. Tel.: +1 217 333 1180; fax: +1 217 244 4333.
E-mail address: aluru@illinois.edu (N.R. Aluru).

0927-0256/$ - see front matter © 2011 Elsevier B.V. All rights reserved.
doi:10.1016/j.commatsci.2011.05.029

Table 1
The Young's modulus of bulk silicon in four typical directions (units: GPa).

Growth direction	MEAM (1992)	MEAM (1999)	Tersoff (1989)	Erhart–Albe	Experimental results	DFT calculations
[1 0 0]	117.39	117.31	88.06, 85 [25]	127.85	131.4 [22]	133.24 [21], 122.8 [24]
[1 1 0]	155.12	123.51	145.14	154.49	169.1 [22]	157.66 [21], 159.4 [20]
[1 1 1]	167.48	127.01	162.35	165.59	187.9 [22]	163.58 [21], 176.6 [20]
[1 1 2]	155.36	124.80	144.83	156.37	160 [23]	168.32 [21]

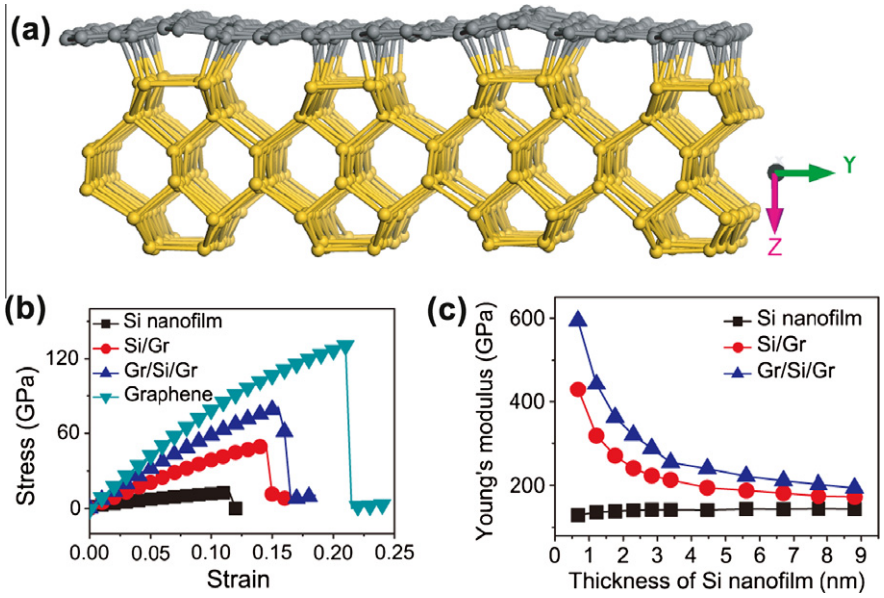

Fig. 1. (a) The relaxed structure for the silicon nanofilm covered with graphene. (b) Stress–strain curves of Si nanofilms, Si/Gr, Gr/Si/Gr, and graphene. (c) The variation of Young's modulus with the thickness of the Si nanofilm for silicon, Si/Gr, and Gr/Si/Gr structures.

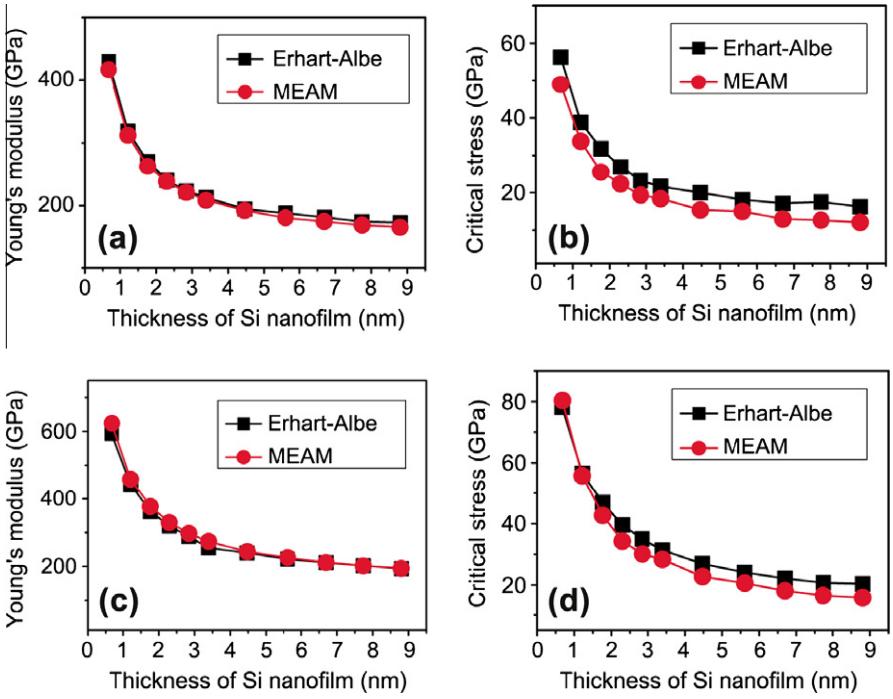

Fig. 2. The variation of Young's modulus with the thickness of the Si nanofilm for Si/Gr (a) and Gr/Si/Gr (c) structures; The variation of critical stress with the thickness of Si nanofilm for Si/Gr (b) and Gr/Si/Gr (d) structures.

300 K and the temperature is controlled by using the Nosé–Hoover thermostat method [19]. The time integration is performed by using the Velocity-Verlet algorithm with an integration time step of 0.1 fs.

3. Results and discussion

We calculate the Young's modulus of bulk silicon at room temperature by performing an NPT ensemble MD simulation. The Young's modulus is evaluated using the expression, $Y = \sigma/\varepsilon$ in the elastic region, where σ and ε are the stress and strain, respectively. Table 1 displays the Young's modulus of bulk silicon for different potentials, and a comparison with previous experimental and theoretical results [20–25] is also shown. As we can see from Table 1, for the [1 0 0] direction, the calculated Young's modulus of bulk silicon using Tersoff (1989) potential is much smaller compared to the experimental result and density functional theory (DFT) calculations. For the [1 1 0], [1 1 1], and [1 1 2] directions, the calculated Young's modulus of bulk silicon using MEAM (1999) potential are much smaller compared to the experimental results and DFT calculations. However, the results from MEAM [17] and Erhart–Albe [15] potentials are in good agreement with previous experimental results and DFT calculations. AIREBO potential has been shown to accurately capture the Young's modulus and fracture strength of bulk graphene [26]. Therefore, we use MEAM (1992) or Erhart–Albe potentials for Si–Si interactions, AIREBO potential for C–C interactions, and Erhart–Albe potential for Si–C interactions in the following study. The silicon atoms on the Si(1 0 0)-2 × 1 surface are initially bonded to the carbon atoms in the graphene. The combined system is fully relaxed until the minimum energy is reached in NPT ensemble. Fig. 1a shows the relaxed structure for the silicon nanofilm covered with graphene. Periodic boundary conditions are used along the *x*- and *y*-directions. In the fully relaxed, stable geometry, each Si atom on the top silicon surface has four bonds. The Si–C bond lengths range from 0.20 nm to 0.22 nm. The Si–C bonds are close to the crystalline SiC bond length (0.19 nm), indicating that the bonding strength of Si–C surface bonds is similar to that of crystalline SiC bonds.

Fig. 1b shows the axial stress–strain curves for silicon nanofilm, Si/Gr (silicon nanofilm covered with graphene on the top surface), Gr/Si/Gr (silicon nanofilm covered with graphene on the top and bottom surfaces), and graphene. The thickness of the silicon nanofilm is 0.67 nm. The thickness of graphene is assumed to be 0.34 nm corresponding to the interlayer spacing in graphite. In this calculation, Erhart–Albe potential is used to describe the Si and Si interactions. The results in the figure indicate that graphene has the highest critical stress and critical strain. Gr/Si/Gr nanofilm has higher critical stress and strain compared to the Si/Gr nanofilm. Si nanofilm has the lowest critical stress and critical strain. The calculated Young's modulus is 946.6 GPa, 594.1 GPa, 430.2 GPa, and 129.4 GPa for zigzag graphene, Gr/Si/Gr, Si/Gr, and Si nanofilm, respectively. The critical stress is 130.6 GPa, 80.9 GPa, 50.8 GPa, and 12.8 GPa for zigzag graphene, Gr/Si/Gr, Si/Gr, and Si nanofilm, respectively. The Young's modulus and critical stress of zigzag graphene are consistent with the experimental results [3]. From the above results, we can see that graphene can enhance the mechanical properties of the silicon nanofilm. The interaction between graphene and the silicon nanofilm and the strong bonding in graphene may be responsible for significant enhancement in the mechanical properties of the silicon nanofilm. In addition, we investigate the effect of the thickness of the silicon nanofilm on the mechanical properties of the silicon, Si/Gr, and Gr/Si/Gr nanofilms, as shown in Fig. 1c. The Young's modulus of the silicon nanofilm increases as the thickness of silicon nanofilm increases, which matches with the previous theoretical results [12]. However, the Young's modulus of Gr/Si/Gr and Si/Gr films decreases as the thickness of silicon nanofilm increases. When the thickness of the silicon nanofilm is 8.81 nm, the Young's modulus of Si/Gr film is 172.9 GPa, which is about 20% higher than that of the silicon nanofilm. The Young's modulus of Gr/Si/Gr film is 193.7 GPa, which is about 35% higher than that of the silicon nanofilm. When the thickness of the silicon nanofilm is 0.67 nm, the Young's modulus of Si/Gr is higher than that of the silicon nanofilm by about 232%. The Young's modulus of Gr/Si/Gr is higher than that of the silicon nanofilm by about 359%. These results indicate that the mechanical property of Si/Gr film depends strongly on the thickness of the silicon nanofilm.

We have also used the MEAM potential to describe the Si and Si interactions. Fig. 2 shows the variation of Young's modulus and critical stress with the thickness of the Si nanofilm for Si/Gr and Gr/Si/Gr structures. The comparison between MEAM and Erhart–Albe potentials is also shown. We observe that both the Young's modulus and critical stress decrease with the increase in thickness

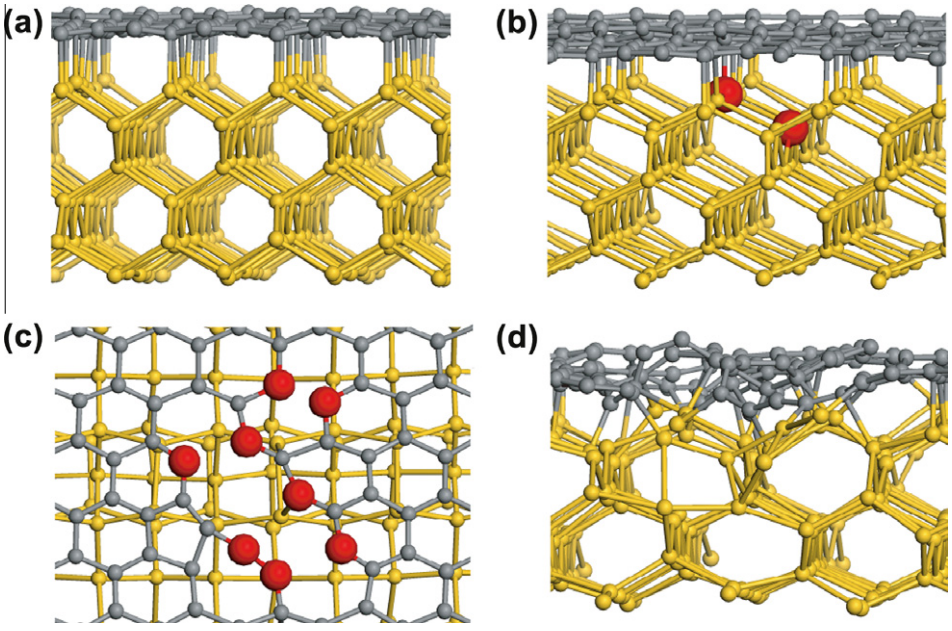

Fig. 3. The atomic configurations of Si/Gr structure for various strains. (a) The strain is 0.05 (side view). (b) The strain is 0.155 (side view, the Si atoms in the broken bond are shown using big red balls). (c) The strain is 0.156 (top view, the C atoms in broken bonds are shown using big red balls). (d) The strain is 0.1565 (side view). (For interpretation of the references to colour in this figure legend, the reader is referred to the web version of this article.)

of the silicon nanofilm. The results from Erhart–Albe and MEAM potentials are also in reasonable agreement with each other.

We also investigated the fracture process of Si/Gr film under tensile loading. Erhart–Albe potential is used to describe the Si and Si interactions. For small strains, as we can see from Fig. 3a, the bonds of Si/Gr film are just stretched and no structural defects appear at this stage. For larger strains, as shown in Fig. 3b, the fracture begins with the breakage of Si–Si bonds near the graphene as the stress reaches critical value. The cohesive energy of bulk silicon, graphene, and bulk SiC are −4.63, −7.73, and −6.34 eV/atom respectively, which indicates that the Si–Si bond is weaker than both C–C bond and C–Si bond.

After the breakage of Si–Si bond, the two regions near the silicon atoms (shown in Fig. 3b by two circles) will move in opposite directions, which will induce an extra stress in graphene. Then the graphene cracks, as shown in Fig. 3c. With a further increase in strain, the whole structure breaks, as shown in Fig. 3d.

4. Conclusions

In summary, in this paper, the mechanical properties of a silicon nanofilm covered with graphene are studied using MD simulations. The predicted Young's modulus of bulk silicon along different directions with Erhart–Albe and MEAM (1992) potentials are consistent with the published theoretical and experimental data. Our results indicate that graphene can enhance the mechanical properties of a silicon nanofilm. The Young's modulus and critical stress of the silicon nanofilm covered with graphene decreases as the thickness of the silicon nanofilm increases. The fracture of silicon nanofilm covered with graphene starts with the breaking of the Si–Si bonds near the graphene.

Acknowledgement

This research was supported by the National Science Foundation under Grant Nos. 0810294 and 0941497

References

[1] X. Li, B. Bhushan, K. Takashima, C. Baek, Y. Kim, Ultramicroscopy 97 (2003) 481.
[2] B. Bhushan, Modern Tribology Handbook, CRC Press, Boca Raton, FL, 2001.
[3] C. Lee, X. Wei, J.W. Kysar, J. Hone, Science 321 (2008) 385.
[4] J. Liang, Y. Huang, L. Zhang, Y. Wang, Y. Ma, T. Guo, Y. Chen, Adv. Funct. Mater. 19 (2009) 2297.
[5] D.W. Wang, F. Li, J.P. Zhao, W.C. Ren, Z.G. Chen, J. Tan, Z.S. Wu, I. Gentle, G.Q. Lu, H.M. Cheng, ACS Nano 3 (2009) 1745.
[6] X. Zhao, Q. Zhang, D. Chen, P. Lu, Macromolecules 43 (2010) 2357.
[7] H. Gleskova, S. Wagner, Appl. Phys. Lett. 79 (2001) 3347.
[8] J. Gaspar, V. Chu, J.P. Conde, Appl. Phys. Lett. 84 (2004) 6622.
[9] Y. Umeno, A. Kushima, T. Kitamura, P. Gumbsch, J. Li, Phys. Rev. B 72 (2005) 165431.
[10] J. Gaspar, O. Paul, V. Chu, J.P. Conde, J. Micromech. Microeng. 20 (2010) 035022.
[11] T. Fujii, Y. Akiniwa, Modelling Simul. Mater. Sci. Eng. 14 (2006) S73.
[12] A.I. Fedorchenko, A. Wang, H.H. Cheng, Appl. Phys. Lett. 94 (2009) 152111.
[13] S. Plimpton, J. Comput. Phys. 117 (1995) 1.
[14] J. Tersoff, Phys. Rev. B 39 (1989) 5566.
[15] P. Erhart, K. Albe, Phys. Rev. B 71 (2005) 035211.
[16] S.J. Stuart, A.B. Tutein, J.A. Harrison, J. Chem. Phys. 112 (2000) 6472.
[17] M.I. Baskes, Phys. Rev. B 46 (1992) 2727.
[18] M.I. Baskes, Mater. Sci. Eng. A 261 (1999) 165.
[19] W.G. Hoover, Phys. Rev. A 31 (1985) 1695.
[20] P.W. Leu, A. Svizhenko, K. Cho, Phys. Rev. B 77 (2008) 235305.
[21] L. Ma, J. Wang, J. Zhao, G. Wang, Chem. Phys. Lett. 452 (2008) 183.
[22] H.J. McSkimin, P. Andreath, J. Appl. Phys. 35 (1964) 2161.
[23] P. Hess, Appl. Surf. Sci. 106 (1996) 429.
[24] B. Lee, R.E. Rudd, Phys. Rev. B 75 (2007) 195328.
[25] Z. Tang, Y. Xu, G. Li, N.R. Aluru, J. Appl. Phys. 97 (2005) 114304.
[26] H. Zhao, K. Min, N.R. Aluru, Nano Lett. 9 (2009) 3012.